

QUANTITATIVE CHARACTERISATION OF CATACLASITES USING A STATISTICAL APPROACH (ANALYSIS OF VARIANCE)

Norbert KOHLMAYER¹ & Bernhard GASEMANN

KEYWORDS

Analysis of variance
Brittle deformation
Cataclasites
Cyclades
Tectonic
D-Value
Aegaen

Department of Geodynamics and Sedimentology, University of Vienna, Althanstraße 14, Vienna, Austria;

¹ Corresponding author, norbert.kohlmayer@aon.at

ABSTRACT

Cataclastic rocks can be described by both a range of shape parameters and the particle size distribution. In this work, we apply statistical methods to investigate these variables in samples with different degrees of maturity from high- and low-angle normal faults within marbles in the W-Cyclades (Greece). Four shape parameters (circularity, elliptical PARIS factor, solidity and the aspect ratio) were used to describe the particles. Using a statistical analysis, the variance of the cataclastic particles of a particular shape is partitioned into fractions attributable to different sources of variation. In addition to the shape parameters, the particle size distribution was included, to test whether there is a relationship between particle size and shape.

The investigations demonstrate that the analysis of variance is a statistical method ideally suited for quantitatively studying the grain-size and shape parameters in cataclasites. Our results indicate that although the particle size distributions of the test samples are very similar, three shape parameters (solidity, circularity and the elliptical PARIS factor) can discriminate between the samples. Ideally, numbers of the shape parameter discretized in individual classes of equivalent diameter of the particle components should be used to quantitatively describe the different samples in order to derive information about the deformation mechanisms in the fault rock. Some of the investigated shape parameters record a clear dependence on the grain-size. In the investigated samples, smaller particles record a higher circularity and a lower elliptical PARIS Factor than larger particles. However, no relationship between the solidity or aspect ratio and the grain size has been observed. This suggests that abrasion and comminution are the dominant deformation mechanism in the finer grained particles but fracturing and cracking are prevalent in the more angular, coarser grained particles.

Kataklasite können mit einzelnen Formparametern der Komponenten respektive mit Verteilungen der Korngrößen der kataklastischen Komponenten beschrieben werden. In dieser Arbeit werden verschiedene Formparameter der Komponenten zusammen mit ihrer Größenverteilung statistisch mit der Varianzanalyse untersucht. Die Methoden wurden an kataklastischen Störungsgesteinen mit unterschiedlichem Reifegrad von steilen und flachwinkligen Störungen in Marmoren aus den W-Kykladen (Griechenland) durchgeführt. Als unabhängige Variablen wurden neben den unterschiedlichen Kataklasiten aus steilen und flachwinkligen Abschiebungen noch die Variable Korngröße in fünf Klassen berücksichtigt. Als abhängige Variable fungierten die Kornformparameter Zirkularität, ein elliptischer PARIS Faktor, Solidität sowie das Achsenverhältnis d.h. das Längen-, Breitenverhältnis der Komponenten. Es sollte die Frage geklärt werden, ob in den verwendeten Proben ein Zusammenhang zwischen Korngröße und Kornform gegeben ist bzw. ob sich die Proben hinsichtlich der Kornformparameter signifikant unterscheiden.

Generell kann gesagt werden, dass die Varianzanalyse eine äußerst geeignete Methode darstellt um Kataklasite quantitative zu beschreiben. Die Untersuchungen an den Testproben erbrachten im wesentlichen folgendes Ergebnis. Obwohl die untersuchten Proben alle eine sehr ähnliche Korngrößenverteilung aufweisen, können sie über die Formparameter Zirkularität, elliptischer PARIS Faktor und Solidität signifikant differenziert werden. Die genannten Kornformparameter diskretisiert in unterschiedliche Korngrößenklassen wurden verwendet um die verschiedenen Proben quantitativ zu beschreiben bzw. daraus Informationen auf die zugrundeliegenden Deformationsmechanismen in den Störungsgesteinen abzuleiten. Ein wichtiger Zusammenhang besteht zwischen den Kornformparametern und der Korngröße da kleinere Komponenten eine höhere Zirkularität und einen geringeren elliptischen PARIS Faktor zeigen als größere Komponenten. Bezüglich Solidität und Achsenverhältnis konnte kein Zusammenhang zur Korngröße festgestellt werden. Zusammenfassend kann für die untersuchten Proben gesagt werden, dass die runderen, kleinen Korngrößen durch Rollen und Abreiben deformiert worden sind, während bei den eckigen größeren Komponenten die Deformation durch Zerbrechen dominiert hat.

1. INTRODUCTION

Cataclasites are fault rocks that form by the mechanical fragmentation of rocks due to microcracking and frictional processes, such as sliding, grinding, and rotation of the fragments

(Passchier and Trouw, 2005 and references cited therein). During cataclastic flow, which may be associated with a dilational component of strain, voids are created that may be filled with

material precipitated from fluids. This material may be subsequently involved in the cataclastic processes (cf. Hausegger et al. 2010). Cataclastic flow usually occurs at non- to low-grade metamorphic conditions and at relatively high strain rates. High fluid-pressures promote cataclastic flow and are responsible for the common occurrence of veins in cataclasites and tectonic breccias (Blenkinsop, 2000 and references cited therein).

All of these processes lead to a particle size distribution (PSD) which is characteristically fractal (e.g., Blenkinsop, 1991). A fractal distribution of particle sizes d can be described by the relation:

$$N(d) \sim d^{-D} \quad \text{Ep. 1}$$

where $N(d)$ is the number of particles greater than size d , and D is the fractal dimension. Since the D-value is used to describe the relationship between grain size and frequency, it is useful to specify the range over which the relationship has a good fit to the data. Truncation, sampling bias and low image resolution effects may lead to the deviation of the large and the small grain sizes from this relationship (Blenkinsop, 1991).

During translation and rotation in cataclastic flow, initially angular fragments may be rounded by fracturing (including grinding and abrasion). Thus an analysis of the progressive shape changes and the spatial rearrangement of the particles during shearing is of great importance (Mair et al., 2002; Storti et al., 2003). Since increasing roundness is a sign of increasing wear, by increasing deformation or displacement, the shape of the fragments can be used to distinguish mature cataclasites (i.e. gouges which have accommodated large displacements) from newly fragmented rocks (Cladouhos, 1999; Storti et al., 2003). It has been suggested that the D-value, in conjunction with shape parameters, can be used to describe cataclastic rocks (Heilbronner and Keulen, 2006) and to correlate this description with the conditions of formation. The present study expands on these ideas and suggests an approach based on a statistical analysis of variance to combine the shape parameters for a quantitative description of cataclastic gouge rocks.

2. SHAPE AND GRAIN SIZE DESCRIPTION OF CATACLASITES

A standard method to describe the frequencies of particle grain sizes in a sample has been described by Blenkinsop (1991); this demonstrated that multiple fracturing of basalts produced a PSD with a higher fractal dimension than a single fracturing event. Grady and Kipp (1987) generalized from experimental data to show that single tensile fragmentation leads to particle size distributions with D-values less than 2, in contrast to shearing and comminution which results in D-values between 2 and 2.4. High D-values, between 2.60 and 2.82, were derived from fault gouges in the Lopes and Witwatersrand faults (Blenkinsop 1991), where PSDs were influenced by lithology (mineralogical composition), fragmentation process, initial size distribution, number of fracturing events and

energy input (Arbiter and Harris, 1965; Hartman, 1969). Some of the earliest experiments on gouge formation (Engelder 1974) showed that the proportion of finer fragments increased with displacement and confining pressure. A reasonably linear reduction in median grain size with increasing confining pressure was recognized for a natural fault gouge in a granodiorite from the San Andreas fault (Sammis et al. 1986). Heilbronner and Keulen (2006) used the D-value to distinguish between cracked fragments from gouge material. Both types of fault rocks exhibit two slopes: for grain size $< 2\mu\text{m}$ $D \sim 1.0$ for both fault rock types; for grain size $> 2\mu\text{m}$, cracked material shows $D \sim 1.6$ while gouge recorded $D > 2.0$.

Image analysis programs were used to automatically derive parameters which describe the size and shapes of the particles (Heilbronner and Keulen, 2006). Two important parameters are the aspect ratio and the PARIS factor. The aspect ratio (ΔR) is defined as the ratio between the longest L and the shortest S projection of a particle. The PARIS factor (Panazzo and Hurlimann, 1983) is a measure of the irregularity of grain boundaries and is defined as the ratio of the perimeter length divided by the outline of the convex hull that envelopes the grain. A smooth grain, such as a circular one or any grain with a convex outline will have a PARIS factor of 1. The value increases as the grain boundary becomes irregular and lobate. Other parameters frequently used are the area, A , and the perimeter, P , of the grains, the circularity C ($C = 4 \pi A/P^2$; a value of 1.0 indicates a perfect circle), the solidity S ($S = A/cA$, where cA is the convex area) and the equivalent diameter $EquiD$ ($EquiD = 2 (A/\pi)^{1/2}$).

3. SAMPLE DESCRIPTION

The two samples examined (Tab. 1) are cataclasites from low- and high-angle normal faults on Kea (W-Cyclades, Greece). The fault system belongs to the West Cycladic Detachment System (Grasemann et al., 2011; Iglseider et al., 2011); this accommodated Miocene extension of the Aegean crust caused by the roll-back of the Hellenic subduction zone (for a regional geological description see the review of Jolivet and Brun 2010). The samples are from cataclastic faults that localized

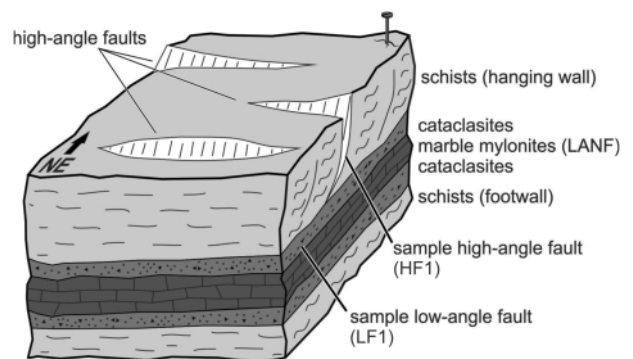


FIGURE 1: Synoptic block diagram showing the interaction of high- and low-angle normal faults (LANF) from the island Kea (Greece). The LANF has a top-to-the SW directed shear sense. Structural location of the two investigated samples HF1 and LF1.

sample	Sample number	GPS coordinates UTM 35	lithology	shear-strain
low-angle fault	LF1	4158684.6/261132.0	marble	high
high-angle fault	HF1	4156750.9/260721.7	marble	low
low-angle fault	LF2	4158684.6/261132.0	marble	high
clast in low-angle fault	CLF2	4158684.6/261132.0	marble	low

TABLE 1: Sample description and sample locations. "high" and "low" shear strains refers to decimeter thick fault rocks, which create an offset in the order of hundreds of meters and a few meters respectively.

in marble host rocks (Fig. 1).

The low-angle faults (analysed image LF1, LF2 and CLF2) represents a brittle segment of a ductile/brittle detachment fault that accommodated displacements in the order of tens of kilometers in total. Although the exact shear-strain taken up by the brittle deformation is unknown, data from other parts of the West Cycladic Detachment System, where a syn-tectonic granodiorite intrusion can be used as a strain marker, suggest that the brittle fault segments accommodated displacements

in the order of 1.5 km (Tscheegg and Grasemann, 2009). The high-angle faults (analysed image HF1) are mechanically linked with the low-angle faults and accommodate extensional strain in the hanging wall of the detachments by bookshelf faulting. The shear strain in such faults is kinematically limited (e.g., Ramsay and Huber, 1987) and marker horizons suggest a few meters to tens of meters of offset. Since we have no better control on the shear strain values, we assume that the shear-strain in the samples from the low-angle fault was "high"

(i.e. in the order of few 100 m to 1 km) and in the high-angle fault was "low" (i.e. in the order 1 m – 10 m). Figure 2 shows two thin-sections of the investigated samples, from which the analysed images were taken.

Low angle fault rocks (LF1, LF2 and CLF2): The ultra-cataclasites from the low-angle normal fault record a random distribution of particles with a size of less than 10 μm to up to 1 cm (Fig. 2a). The calcitic matrix has a dark brown colour containing angular to rounded fragments that consists of either aggregates of dolomite crystals, single dolomite and calcite crystals or dolomite cataclasites. Generally, the dolomite cataclasite fragments are more rounded than the dolomite aggregates, suggesting reworking of fault rocks within the cataclasites by abrasive wear. The dolomite aggregates break either along the grain boundaries or along the cleavage of the dolomite crystals. Locally, a spaced pressure solution cleavage and micro-veins, filled with calcite, indicate dissolution-precipitation processes. Some of the calcite veins record strong overprinting by deformation twinning and by frictional deformation, suggesting that the calcite fragments in the cataclasites are a reworked filling of the veins. In general, the microstruc-

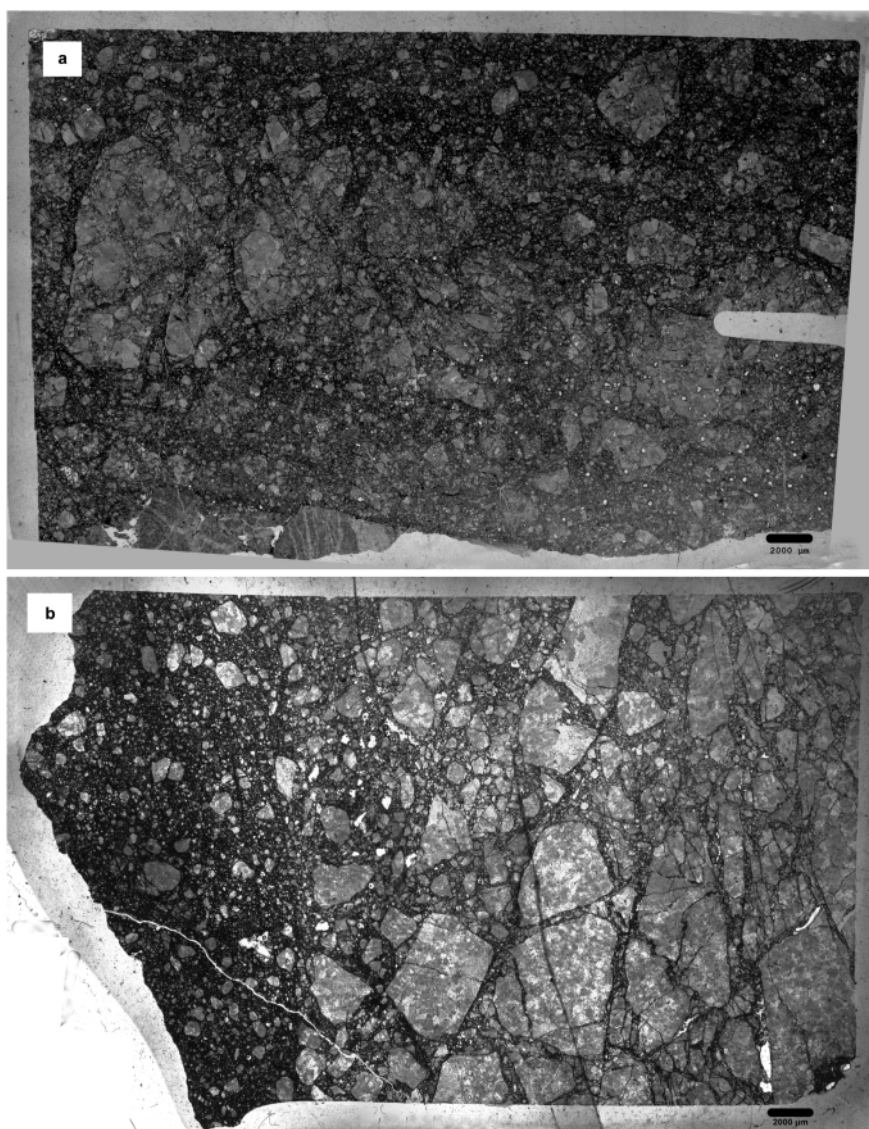


FIGURE 2: Microstructure of cataclasite from low-angle fault (a); and high-angle fault (b).

tures suggest alternating periods of cataclastic flow dominated by fracturing, translation and grinding of particles (velocity weakening) and periods of dissolution precipitation creep (velocity hardening). LF1 and LF2 are from the ultracataclasites and CLF2 is a cataclastic component in LF2.

High angle fault (HF1): The investigated thin section records two different parts: (i) a protocataclastic zone (central and right part in Fig. 2b) and (ii) an ultracataclastic zone (left part in Fig. 2b). The protocataclasites are characterized by cm size dolomite host-rock components with extensive microfractures. The much finer grained ultracataclastic material with a dark brown calcite matrix and with a random fabric was injected into fractures and voids that developed between the dolomitic host rock particles, especially in the transition zone between the ultracataclasite and the protocataclasite. In the ultracataclasite zone, the largest components are less than 2 mm in size and are angular to partly rounded. The particles consist of dolomite single crystals and aggregates similar to the larger protocataclastic components. No counterparts of fractured particles have been observed. No cataclastic particles occur in the ultracataclasite and no evidence for dissolution precipitation creep is observed. Our interpretation is that these fault rocks formed by fluidization processes; this would explain the random fabric, the injection structures and the missing counterpart particles (Monzawa and Otsuki, 2003). HF1 is from the ultracataclastic zone.

4. DATA ACQUISITION

Electron microprobe backscattered electron (BSE) images were acquired on a Cameca SX-100 electron microprobe (Department of Lithospheric Research, University of Vienna). Methods and measurement conditions are described in Tschegg and Grasmann (2009). Representative parts of the BSE images of samples LF1, LF2, HF1 and CLF2 were analysed

with the program ImageJ (rsbweb.nih.gov/ij/). Due to the different grey shadings of the dolomite clasts and the calcitic matrix in the BSE images, the particles were automatically detected using a color coded filter (Fig. 3a).

All particles smaller than 19 μm were then deleted because of resolution effects influencing further statistical analysis (Fig. 3b).

For each remaining particle, the following parameters were automatically calculated (length and area parameter are measured in μm and μm^2 respectively): Area A , Perimeter P , aspect ratio AR , circularity C , solidity S and equivalent diameter $EquiD$. In contrast to the PARIS factor of Panazzo and Hurlimann (1983), we calculated an elliptical PARIS factor EP , which is the difference between the perimeter of a particle and the perimeter of a fit-ellipse envelop P_{ell} of the particle ($EP = (P - P_{ell})/P_{ell}$).

For further statistical data analysis, we used the multivariate statistics software package SPSS (www.ibm.com/software/at/analytics/spss/products/statistics). Before further processing, 5 classes of equivalent diameter were generated for samples LF1, LF2, HF1 and CLF2. In particular, the particles of the samples were divided in 5 classes of diameter with minimum and maximum diameter and number of particles (Tab. 2; see also box-plots Appendix A in the electronic supplement). Based on this, SPSS tables including all parameters derived by the automatic image analysis were compiled. A template of such an SPSS table is given in Appendix C in the electronic supplements.

5 METHOD AND IMPLEMENTATION OF DATA ANALYSIS

As outlined above, the investigated samples clearly had a different tectonic history in terms of deformation mechanism and finite strain. Using a quantitative statistical approach, the following questions could be addressed:

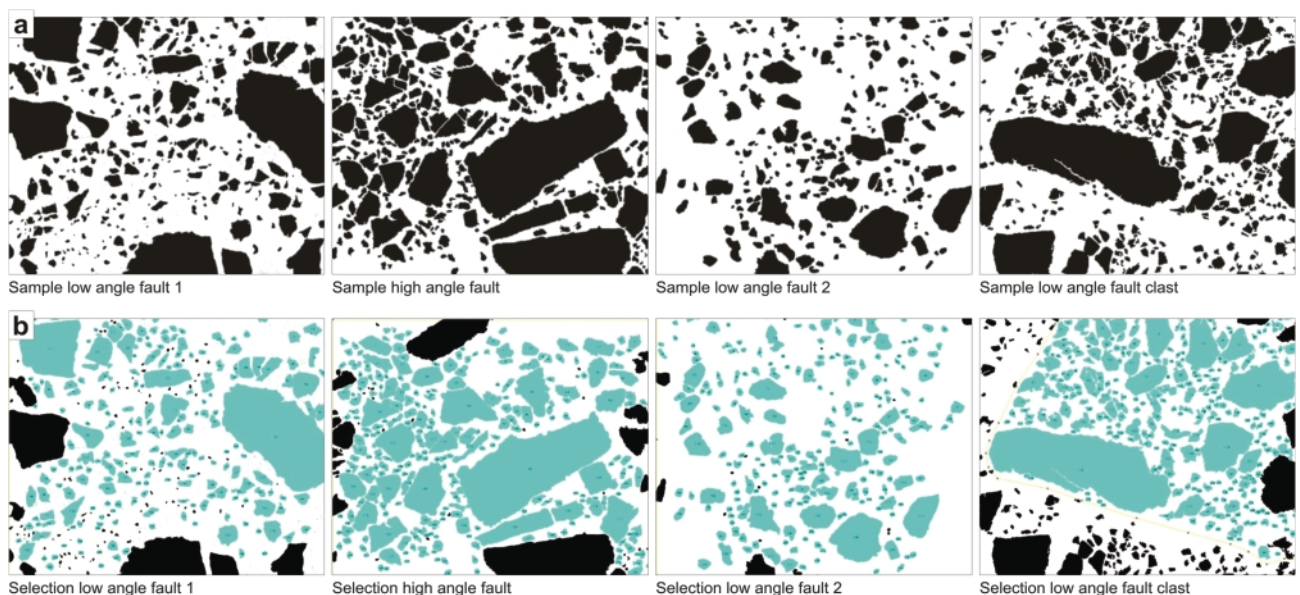


FIGURE 3: a: Automatic detected particles from the BSE images using the program ImageJ. b: Selection of particles with a grain size > 19 μm and exclusion of particles, which are cut by the border of the image.

		Sample											
		LF1			HF1			LF2			CLF2		
		EquiD			EquiD			EquiD			EquiD		
		Minimum	Maximum	Count									
Classes of equivalent diameter	1	19.09	24.54	40	19.21	25.22	34	19.59	24.84	35	19.04	25.07	80
	2	25.51	32.54	35	25.32	32.61	44	25.32	32.61	52	25.26	32.69	57
	3	32.76	42.73	41	32.76	42.73	52	33.06	42.56	44	32.84	42.81	52
	4	43.02	65.26	46	43.91	65.60	58	43.07	66.33	46	43.26	65.34	38
	5	66.92	590.75	45	66.81	663.82	56	66.48	298.30	44	66.66	652.72	43
	Total	19.09	590.75	207	19.21	663.82	244	19.59	298.30	221	19.04	652.72	270

TABLE 2: Classification of the equivalent diameter for particles > 19 µm in samples LF1, LF2, HF1 and CLF2.

- Is there a significant difference in the shape parameters (circularity, aspect ratio, solidity and elliptical PARIS factor) between samples of different tectonic history?
- Is there a significant difference between the five equivalent diameter classes in all specific questions above?
- Are there significant interactions between tectonic history and classes to equivalent diameter?

5.1 THEORY OF THE VARIANCE ANALYSIS:

“...In investigations in which many factors are involved, it will not be economic or efficient to investigate the effect of one factor at a time on the particular result under investigation. Such a procedure gives no information about the possible interactions which may exist between relevant factors.” (Huitson, 1966).

In this work, the variance analysis is applied using two factors, the factor tectonic (i.e. samples from the high- and low-angle normal fault deformed by different deformation mechanisms) and the factor grain-size. For the factor grain-size, five classes are used, based on which model equations can be formulated (Backhaus et al., 1996; Field, 2005). For example the equation for the dependent variable y_{ghk} :

$$y_{ghk} = \mu + \alpha_g + \beta_h + (\alpha\beta)_{gh} + e_{ghk} \quad \text{Eq. 2}$$

Where the index g represents the samples (1-4), h is the number of grain-size classes (1-5) and k represents the number of investigated particles in each section. This equation states that, for example, the circularity of a particle y_{ghk} , is caused by an overall mean value μ , plus the effect of the g^{th} level of factor A (e.g. tectonics) plus the effect of the h^{th} level of factor B (e.g. grain-size), plus the gh^{th} interaction between factor A and factor B (e.g. tectonics with grain size). The interaction $(\alpha\beta)$ indicates an effect that acts in addition to the isolated main effects α and β (see Bortz, 1999). The term e_{ghk} takes into account all those factors which have not been included in the study. The partition of one observation into different cases of influence can be assigned to the total variability of a set of data

$$SS_t = SS_A + SS_B + SS_{A \times B} + SS_W \quad \text{Eq. 3}$$

where SS_A is the sum of squares of factor A (e.g. tectonics), SS_B is the sum of squares of factor B (e.g. grain-size), $SS_{A \times B}$ is the sum of squares caused by the interaction of factor A and B and SS_W is the residual sum of squares.

To find the total amount of variation within the data, we calculate the difference between each observed data point y_{ghk} and the grand mean \bar{Y} . The squared differences were added resulting in the total sum of squares (SS_t):

$$SS_t = \sum_{g=1}^G \sum_{h=1}^H \sum_{k=1}^K (y_{ghk} - \bar{Y})^2 \quad \text{Eq. 4}$$

where G is the number of levels of factor A, H is the number of levels (classes) of factor B and K is the number of observations combining factor A and B.

The model sum of squares SS_M unites three components:

$$SS_M = SS_A + SS_B + SS_{A \times B} \quad \text{Eq. 5}$$

SS_M is calculated from the data with the difference between each group mean and the overall mean.

$$SS_M = K \sum_{g=1}^G \sum_{h=1}^H (\bar{y}_{gh} - \bar{Y})^2 \quad \text{Eq. 6}$$

SS_A represents the variation of the data controlled by the contrasting tectonic history.

$$SS_A = H \cdot K \cdot \sum_{g=1}^G (\bar{y}_g - \bar{Y})^2 \quad \text{Eq. 7}$$

SS_B describes the variation in data controlled by the different grain sizes.

$$SS_B = G \cdot K \cdot \sum_{h=1}^H (\bar{y}_h - \bar{Y})^2 \quad \text{Eq. 8}$$

Finally, the interaction effect $SS_{A \times B}$ represents the variance controlled by interaction of the two variables (tectonic history and grain size). This can be calculated very easily, because $SS_M = SS_A + SS_B + SS_{A \times B}$ (see above).

$$SS_{A \times B} = SS_M - SS_A - SS_B \quad \text{Eq. 9}$$

The residual sum of squares SS_W represents the effects of

variations, which cannot be explained by the model.

$$SS_W = SS_t - SS_M \tag{Eq. 10}$$

To find the average amount of variation explained by the model, SS_A , SS_B , SS_{AxB} and SS_W must be divided by the degrees of freedom (Backhaus et al., 1996). With these values, the F-ratio can then be calculated (Field, 2005).

The F-ratio is a measure of the ratio of the variation explained by the model and the variation explained by unsystematic factors. If this value is less than 1 then it represents a non-significant effect (i.e. more unsystematic than systematic variance). If the F-value is greater than 1 it means that the systematic effect is greater than the unsystematic effect, but it is not constrained whether this is a chance result. In order to test this, the F-value is compared with the maximum random value in an F-distribution with the same degrees of freedom.

5.2 DATA PROCESSING WITH SPSS

The univariate analysis of variance was calculated with the software SPSS; this firstly gathers descriptive statistical information from the sample data and secondly tests the validity of the calculation and the precondition (for the assumptions and a SPSS output and example datafile see Appendices B, C and D in the electronic supplement). The full output file of the SPSS calculations is provided in the electronic supplements. In this, the mean results for every dependent variable are separately shown in several tables as well as graphically. Table 3 shows an example for the Test of *Between-Subjects Effects* for the circularity. The first and the last columns are important in this table. Columns 2 to 5 show the sum of squares, the degree of freedom *df*, the mean square and the F-value. The last column *Sig* shows the probability that the observed results come about only under the condition chance. Generally, probabilities smaller than 0.05 are considered to be significant; that is, the observed results have only a 5% probability of being random.

6. RESULTS OF THE ANALYSIS OF VARIANCE

6.1 CIRCULARITY, SAMPLE AND EQUIVALENT DIAMETER

Table 3 shows in the column “source” and “Sig” that for Model, Sample and EquiDclasses, the probability for a random result is smaller than 0.000. The first row with the entry Model indicates that the calculation with the used dependent and independent variables throughout is sig-

nificant with 0.000. The subsequent rows, with the entry Sample and EquiDclasses, mean that the possibility for the differences in the circularity between the factor levels of the samples and the factor levels of the diameter classes under the condition chance are also very low. In contrast, the interaction “Sample * EquiDclasses” is under the condition chance possible in 40% percent of the cases.

The effect size of the model is the ratio of model sum of square (Corrected Model) to total sum of square (Corrected Total). It is 40.1% for the variable Circularity. That means 40% of the total sum of square (Corrected Total) is explained by the model. This percentage is divided equally between the sample and grain size. The 60% of the variance that is not explained was caused by factors which were not considered here (Backhaus et al., 1996).

The subsequent calculated *Post Hoc Test* (Table 7) highlights those samples that differ significantly from the others. In this case, the samples are grouped by their circularity. It can be seen that samples HF1 and CLF2 belong to the same group because the circularities of these samples are very similar. However, all the other samples are classified in separate groups.

The grouping of the samples in terms of the measured circularity can be visualized in a plot of the estimated means of the circularity for each sample versus the class of equivalent diameter (Fig. 4). This clearly shows the close relationship between samples HF1 and CLF2. In contrast, samples LF1 and LF2 represent separate classes with generally higher circularities. However, the plot also demonstrates that for all samples there is a clear trend of the circularity to decrease

Tests of Between-Subjects Effects					
Dependent Variable: Circ.					
Source	Type III Sum of Squares ¹	df	Mean Square	F	Sig.
Corrected Model	11.145 ^a	19	.587	32.533	.000
Intercept ²	335.915	1	335.915	18630.158	.000
Sample	6.034	3	2.011	111.545	.000
EquiDclasses	5.026	4	1.257	69.691	.000
Sample * EquiDclasses	.226	12	.019	1.045	.405
Error	16.624	922	.018		
Total	373.184	942			
Corrected Total	27.770	941			

a. R Squared = .401 (Adjusted R Squared = .389)

TABLE 3: Test of Between-Subjects Effects for the dependent variable circularity

¹ The column “Type III Sum of Squares” means that the sum of squares were adapted to the fact that not all cells of the model are equal full. In the 4x5 cells (4 samples and 5 Equidclasses) the amount of components are not equal.

² The value of the intercept is for the interpretation not important, reason for this entry is that SPSS performs the calculation with a regressions analysis.

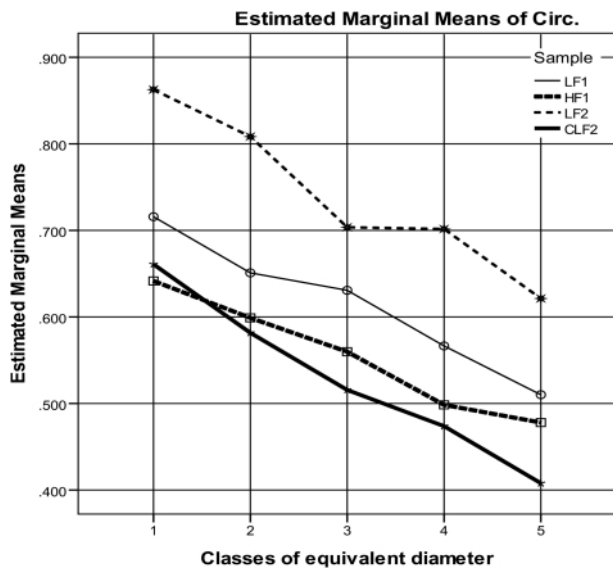


FIGURE 4: Diagram of the circularity versus the classes of equivalent diameters for the four investigated sample.

with higher equivalent diameter classes.

6.2. ASPECT RATIO, SAMPLE AND EQUIVALENT DIAMETER

Table 4 shows that with respect to the dependent variable aspect ratio, only the samples record significant differences but the classes of diameter do not differ significantly. The interaction between the two factors sample and equivalent diameter classes with a value of 0.059 is also not significant. The post hoc test (Tab. 7) demonstrates that the significance of the sample value in Table 4 is dominated by the aspect ratio value of LF2. The value of this sample is the lowest in all classes of equivalent diameters and is therefore classified into a single group. The three other samples form a second group.

The plot of the aspect ratio versus the classes of equivalent diameters for the four investigated samples (Fig. 5) shows that LF2 differs from the other three samples, which record higher aspect ratios. Whereas HF has higher aspect ratios of the particles in the coarser classes of equivalent diameters, LF1 and CLF2 have unsystematically scattered aspect ratios. Therefore, the effect size for the variance of the aspect ratio is only 5% of the total variance.

6.3 SOLIDITY, SAMPLE AND EQUIVALENT DIAMETER

The parameter solidity (the ratio of area to convex area), shows significance only dependent on the sample factor (Tab. 5), but as highlighted by the post hoc test, there are great differences between the samples (Tab. 7). In fact, the results of the post hoc test suggest that all samples strongly differ from each other and that all the samples have to be classified into separate groups. This can be visualized in a plot of the solidity versus the classes of equivalent diameters for the four samples (Fig. 6). The solidity of the particles in all samples records a minor variability and unsystematically scatters in the different classes of equivalent diameter. However, the four samples can be clearly distinguished using the solidity of their particles, with particles from LF2 recording the highest solidity.

The model effect for the dependent variable solidity is 19% which is only influenced by the factor sample. The factor grain size effects only 0.8% of the variance.

6.4 ELLIPTICAL PARISFACTOR, SAMPLE AND EQUIVALENT DIAMETER

The statistical test Between-Subject Effects clearly demonstrates that all factors as well as the interaction between the factors are significant (Tab. 6). Similarly, the post hoc test (Tab. 7) allows a clear grouping of the samples where HF1 and CLF2 record the closest relationships (i.e. they belong to the same group). All other samples are classified in individual groups.

The plot in Figure 7 shows the elliptical PARIS factor versus the classes of equivalent diameters. It can be seen that in all four investigated samples the elliptical PARIS factor of the particles increases with the classes of equivalent diameter. The larger the grain size, the more irregular the particle boundaries become. CLF2 and HF1 form the group with the greater values in the elliptical PARIS Factor and have more irregular particle boundaries compared to smoother particles of LF1 and LF2.

The model effect for the Elliptical PARIS Factor is 36%, which is influenced by sample and grain size

Tests of Between-Subjects Effects					
Dependent Variable:AR					
Source	Type III Sum of Squares	df	Mean Square	F	Sig.
Corrected Model	19.243 ^a	19	1.013	2.792	.000
Intercept	2825.163	1	2825.163	7786.803	.000
Sample	10.076	3	3.359	9.257	.000
EquiDclasses	1.852	4	.463	1.276	.278
Sample * EquiDclasses	7.469	12	.622	1.716	.059
Error	334.515	922	.363		
Total	3342.419	942			
Corrected Total	353.758	941			

a. R Squared = .054 (Adjusted R Squared = .035)

TABLE 4: Test of Between-Subjects Effects for the dependent variable aspect ratio AR.

in approximately equal amounts.

7. DISCUSSION

The particle size distribution in cataclasites can be quantified using the D-value (Eq. 1), which provides information about the frequency of particle sizes for a particular particle size range. Many processes that lead to the formation of cataclastic fault rocks, such as mechanical fragmentation, microcracking, sliding, grinding or spalling of the fragments, result in different particle size distributions, which are further complicated by mineralogical phases, chemomechanical feedback processes and the finite strain (e.g. Blenkinsop and Rutter, 1986; Sammis et al., 1986; Marone and Scholz, 1989; An and Sammis, 1994; Monzawa and Otsuki, 2003; Rawling and Goodwin, 2003; Billi 2005; Keulen et al., 2007; Stünitz et al., 2010). However, in most studies, the dominant process of cataclasis under lithostatic compaction or shear deformation has been observed to be transgranular fracturing initiated by loading at grain-to-grain contacts abrasion with additional flaking or spalling from grain edges. Therefore, cataclastic fault rocks generated in the laboratory, preferentially record D-values at about 2.5–2.6 (Sammis et al., 1986; Biegel et al., 1989; Marone and Scholz, 1989; Billi and Storti, 2004) suggesting scale and time invariance of the fragmentation processes. However, other studies present evidences indicating that D-values systematically increase from immature to mature cataclastic rocks (Marone and Scholz, 1989; Hattori and Yamamoto, 1999; Storti et al., 2003; Billi and Storti, 2004). Relating the maturity of cataclasites with finite strain in the brittle fault zone, the observed systematic variation in D-values suggests that the dominant particle fragmentation mechanism changes and the contribution of chipping and surface abrasion increases with progressing particle interaction (Hattori and Yamamoto, 1999; Storti et al., 2003).

The PSD of our samples (Fig. 8) records D-values that are in good agreement with other published D-values for natural and experimental fault rocks (e.g., Heilbronner and Keulen, 2006). Although we are aware of the problems of this technique because of the sensitivity to cut-off effects at large sizes, there is little variation in the D-values between the investigated samples (LF1: 1.7; LF2: 1.8; CLF2: 1.7; HF1: 1.5, see Fig. 8), in agreement with the proposed scale and time invariance of the fragmentation processes. A detailed discussion about the D-value and its validity is given in Hergarten (2002). A number of other studies focused on the shape parameters of particles, to unravel processes during cataclastic deformation. It has

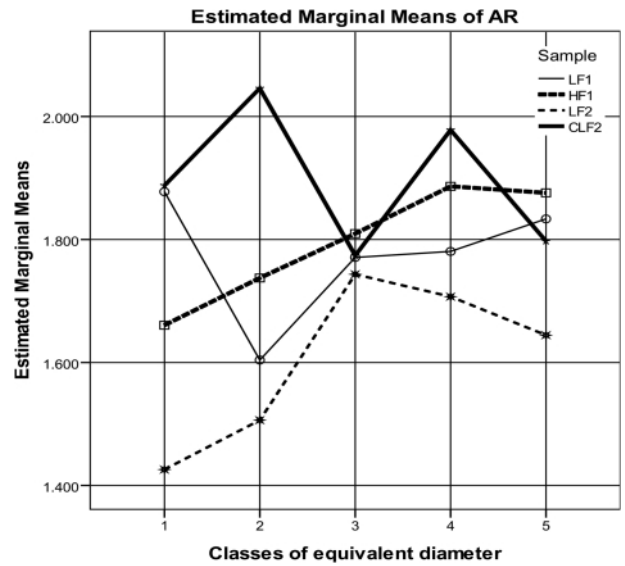


FIGURE 5: Diagram of the aspect ratio versus the classes of equivalent diameters for the four investigated sample.

been shown, for example, that a microstructural analysis of the fragment shapes shows a dependency on the amount of slip and may record some information on slip magnitude. With increasing displacement, grain shapes evolve towards more rounded and less serrated grains, while the grain size distribution remains constant (Mair and Marone, 1999; Heilbronner and Keulen, 2006; Storti et al., 2007; Stünitz et al., 2010).

However, in most of these studies the particle shape parameters were mainly evaluated individually or compared with the statistic averages of each individual sample. A quantitative interpretation of the shape values is difficult since without statistical tests it is impossible to establish which trends are significant and which can be regarded as coincidental.

Tests of Between-Subjects Effects					
Dependent Variable: Solidity					
Source	Type III Sum of Squares	df	Mean Square	F	Sig.
Corrected Model	1.013 ^a	19	.053	11.670	.000
Intercept	637.609	1	637.609	139572.707	.000
Sample	.928	3	.309	67.735	.000
EquiDclasses	.042	4	.011	2.302	.057
Sample * EquiDclasses	.048	12	.004	.874	.573
Error	4.212	922	.005		
Total	666.055	942			
Corrected Total	5.225	941			

a. R Squared = .194 (Adjusted R Squared = .177)

TABLE 5: Test of Between-Subjects Effects for the dependent variable solidity.

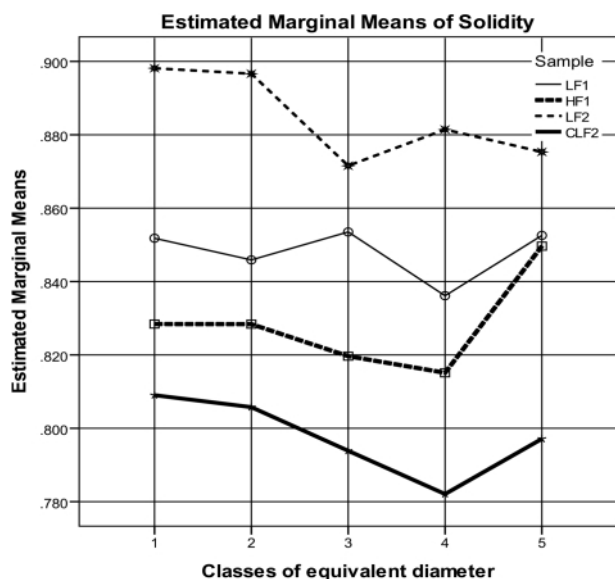


FIGURE 6: Diagram of the solidity versus the classes of equivalent diameters for the four investigated sample.

The presented analysis of variance provides more robust information than the simple statistical analysis of data series. The main advantage of the analysis of variance presented here is that, firstly, the indicators can be tested for random influences, and, secondly, multiple parameters (e.g. measured shape factors) enter in the analysis simultaneously and, therefore, mutual influences and known interactions can be detected. The statistical methods used here investigate the sample and the effect of grain-size in relation to the particle shape parameters and therefore it can be quantified whether or not a particular sample in a given particle size shows random or significant trends in relation to grain-shape parameters.

The analysis of variance clearly demonstrated significant differences between the distribution of some particle sizes in re-

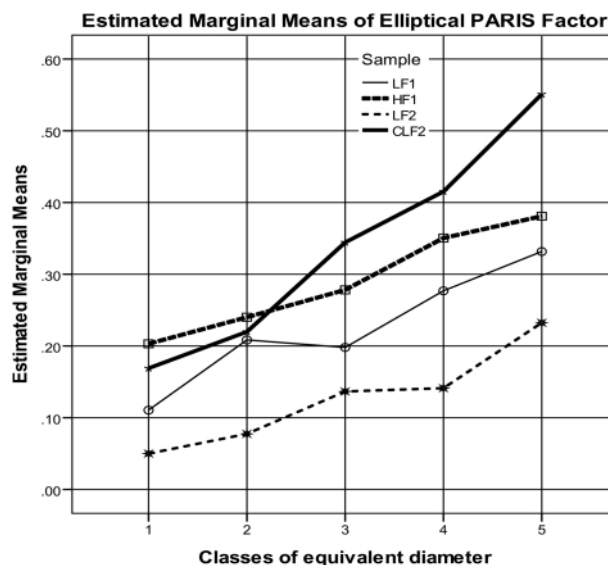


FIGURE 7: Diagram of the elliptical PARIS Factor versus the classes of equivalent diameters for the four investigated sample.

lation to the various shape parameters, in the investigated samples and between the samples. The statistical analysis presented clearly provides additional information that can help to quantitatively discriminate between similar and dissimilar cataclastic fault rocks. Further, it can also provide information about the deformation mechanisms that controlled the formation of the cataclasites.

In the following, we present a short and cautious interpretation of the PSD in combination with the statistically investigated shape parameters of the studied samples:

The circularity and elliptical PARIS factor are well suited for distinguishing between the different samples and show a clear trend in the investigated grain-sizes. In all samples, there is a decrease in circularity with increasing grain-size classes. Similarly, there is an increase in the elliptical PARIS factor with increasing grain-sizes. HF1 and CLF2 show very similar trends and record less circular particles (and higher elliptical Paris factor) than the samples LF1 and LF2; this probably reflects the higher maturity (higher finite strain) of the samples from the low-angle faults. In the early stages of brittle fault development, particle fragmentation is the dominant mechanism resulting in coarse and angular particles. With progressing deformation, particle interaction by rolling, sliding and rotation favours surface abrasion and chipping (i.e. grinding) that eventually become the dominant deformation mechanisms resulting in more rounded grains (Biegel et al., 1989; Blenkinsop, 1991; Hattori and

lately, there is an increase in the elliptical PARIS factor with increasing grain-sizes. HF1 and CLF2 show very similar trends and record less circular particles (and higher elliptical Paris factor) than the samples LF1 and LF2; this probably reflects the higher maturity (higher finite strain) of the samples from the low-angle faults. In the early stages of brittle fault development, particle fragmentation is the dominant mechanism resulting in coarse and angular particles. With progressing deformation, particle interaction by rolling, sliding and rotation favours surface abrasion and chipping (i.e. grinding) that eventually become the dominant deformation mechanisms resulting in more rounded grains (Biegel et al., 1989; Blenkinsop, 1991; Hattori and

Tests of Between-Subjects Effects					
Dependent Variable: Elliptical PARIS Factor					
Source	Type III Sum of Squares	df	Mean Square	F	Sig.
Corrected Model	12.984 ^a	19	.683	27.613	.000
Intercept	54.632	1	54.632	2207.560	.000
Sample	5.815	3	1.938	78.325	.000
EquiDclasses	6.285	4	1.571	63.491	.000
Sample * EquiDclasses	1.108	12	.092	3.732	.000
Error	22.818	922	.025		
Total	93.445	942			
Corrected Total	35.801	941			

a. R Squared = .363 (Adjusted R Squared = .350)

TABLE 6: Test of Between-Subjects Effects for the dependent variable elliptical PARIS factor.

Yamamoto, 1999). Additionally, the efficiency of particle cracking decreases with decreasing grain-size and therefore smaller particles get more rounded by continuous abrasion (Blenkinsop, 1991). Rounded particles accommodate shear mainly by rolling resulting in fault weakening, i.e. the progressive decrease in friction with increasing fault displacement (Mair et al., 2002; Guo and Morgan, 2004; Anthony and Marone, 2005). Interestingly, Storti et al. (2007) presented data from carbonate cataclases that show that particle angularity systematically decreases with increasing particle size and with increasing fractal dimension. The evidence that smaller particles are more angular than larger ones was interpreted to indicate a deformation process where particle fragmentation dominates in the early evolutionary stages of the fault, while comminution and spalling control cataclasis at higher of fault displacements.

Generally, fracturing of grains produces higher aspect ratios, which is further controlled by the mineralogical composition (Heilbronner and Keulen, 2006), although the shape anisotropy of the particles may be also an inherited feature, associated with the orthorhombic symmetry of joint patterns, which enhances fracturing of lithons perpendicular to their long symmetry axes (e.g. Engelder, 1987; Ramsay and Lisle, 2000; Billi et al., 2004). The aspect ratio of particles in cataclases is significantly influenced (increased) by dissolution-precipitation processes (Babaie et al., 1991; Stünitz et al., 2010; Rowe et al., 2011). In the investigated samples, the aspect ratio shows no systematic trends and is independent on the classes of equivalent diameter.

The solidity, which has rarely been used as a shape parameter in quantifying particle structures in cataclases, gives information about the roughness or smoothness of particle edges. The solidity in the investigated particle shapes clearly separates the samples into four different groups. The order of separation is the same as that derived by the circularity and elliptical PARIS factor, highlighting the relationship between roundness and smoothness of particle borders. In contrast to the circularity and the elliptical PARIS factor, the solidity is nearly insensitive to the classes of equivalent diameters.

To our knowledge, the present study is the first application of the well established statistical method of variance analysis to quantitatively investigate the grain-size and shape parameters of cataclases. To test this method, we selected samples from marble cataclases, where only the influence of the grain-size on the particle shape parameters and their interactions were investigated. The method can be easily extended in future to fault rocks that consist of different mineralogical particles, which may have a significant influence of grain-size and particle shape parameters.

8. CONCLUSIONS

1) The analysis of variance is a powerful statistical method that can be applied to quantitatively investigate the grain-

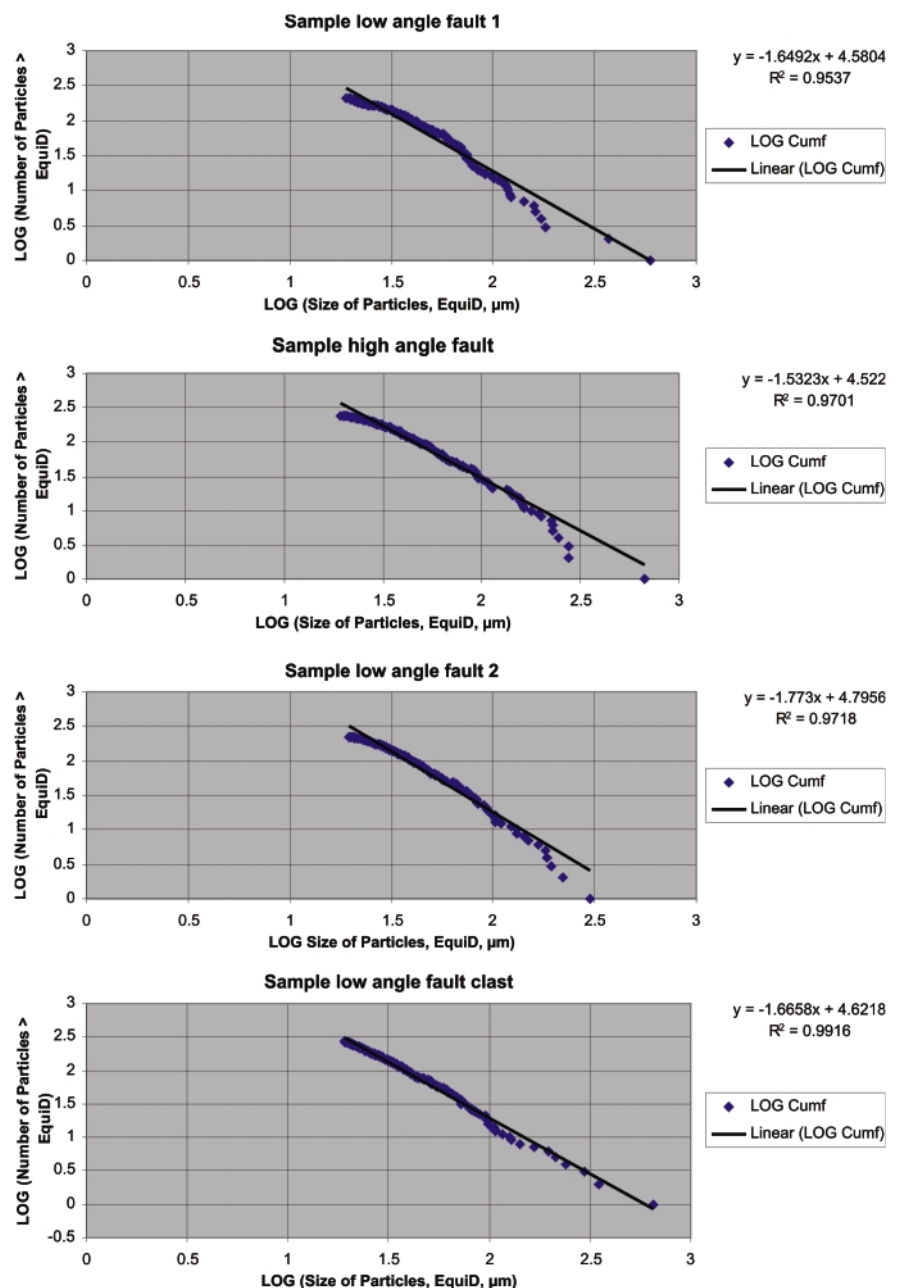


FIGURE 8: Log-Log diagram of particle size versus number of particles. The absolute value of the slope of the regression line corresponds to the D-value. a) LF1; b) HF1; c) LF2; d) CLF2

Results: Post Hoc Tests	SAMPLE			
	CLF2	HF1	LF1	LF2
Circularity 1	0.55	0.54		
Circularity 2			0.61	
Circularity 3				0.74
AR 1				1.61
AR 2	1.89	1.81	1.77	
Solidity 1	0.79			
Solidity 2		0.82		
Solidity 3			0.85	
Solidity 4				0.88
EII. PARIS-f 3	0.31	0.30		
EII. PARIS-f 2			0.23	
EII. PARIS-f 1				0.13

TABLE 7: Post Hoc Tests. The test after the analysis of variance in order to group the samples according to their values of circularity, aspect ratio (AR), solidity and elliptical PARIS factor (EII. PARIS-f).

size and particle shape parameters of cataclasites.

- 2) Four test samples from low- and high-angle faults in the Western Cyclades representing fault rocks that were formed by different deformation mechanisms and accommodated different finite strains, record partly very different particle shape parameters but similar particle-size distributions.
- 3) In the test samples, circularity and the elliptical PARIS factor show systematic trends in the classes of equivalent diameters. The finer grained particles are more rounded suggesting that abrasion and comminution was the dominant deformation mechanism in comparison to the more angular, coarser-grained particles, where fracturing prevailed.
- 4) Solidity, which is similar to circularity and the elliptical PARIS factor, which is also a function of the roundness of the particles, shows no dependence on the classes of equivalent diameters, emphasizing the need to analyzing a broad variation of particle shape parameters.
- 5) The present study identified the circularity, the elliptical PARIS factor and the solidity as useful shape parameters for discriminating between the different samples.

ACKNOWLEDGEMENTS

We thank Christoph Iglseder for providing the investigated samples from Kea including the thin sections and the BSE images and for discussions about the geology of Kea and the Aegean region. Two reviews by S. Hergarten and W. Kurz and handling of the manuscript by W. Kurz, Associate Editor

of the Austrian Journal of Earth Sciences, are gratefully acknowledged. Hugh Rice significantly improved the language and style of the manuscript.

REFERENCES

- An, L.-J., Sammis, C.G., 1994. Particle size distribution of cataclastic fault materials from Southern California: A 3-D study. *Pure and Applied Geophysics*, 143, 203-227.
- Anthony, J.L. and Marone, C., 2005. Influence of particle characteristics on granular friction. *Journal of Geophysical Research*, 110, B08409.
- Arbiter, N. and Harris, C.C., 1965. Particle size distribution time relationships in comminution. *British Chemical Engineering*, 10, 240-247.
- Babaie, H.A., Babaei, A. and Hadizadeh, J., 1991. Initiation of cataclastic flow and development of cataclastic foliation in non-porous quartzites from a natural fault zone. *Tectonophysics*, 200, 67-77.
- Backhaus, K., Erichson, B., Plinke, W. and Weiber, R., 1996. *Multivariate Analysemethoden*. Springer-Verlag, Berlin Heidelberg New York, 591 pp.
- Billi, A. and Storti, F., 2004. Fractal distribution of particle size in carbonate cataclastic rocks from the core of a regional strike-slip fault zone. *Tectonophysics*, 384, 115-128.
- Billi, A., 2005. Grain size distribution and thickness of breccia and gouge zones from thin (<1 m) strike-slip fault cores in limestone. *Journal of Structural Geology*, 27, 1823-1837.
- Biegel, R.L., Sammis, C.G. and Dieterich, J.H., 1989. The frictional properties of a simulated gouge having a fractal particle distribution. *Journal of Structural Geology*, 11, 827-846.
- Bjork, T.E., Mair, K. and Austrheim, H., 2009. Quantifying granular material and deformation: Advantages of combining grain size, shape, and mineral phase recognition analysis. *Journal of Structural Geology*, 31, 637-653.
- Blenkinsop, T.G. and Rutter, E.H., 1986. Cataclastic deformation of quartzite in the moine thrust zone. *Journal of Structural Geology*, 8, 669-681.
- Blenkinsop, T., 1991. Cataclasis and processes of particle size reduction. *Pure and Applied Geophysics*, 136, 59-86.
- Blenkinsop, T., 2000. *Deformation Microstructures and Mechanisms in Minerals and Rocks*. Kluwer Academic Publishers, Dordrecht Boston London, 150 pp.
- Bortz, J., 1999. *Statistik für Sozialwissenschaftler*. Springer-Verlag, Berlin, Heidelberg, New York, 836 pp.

- Cladouhos, T.T., 1999. Shape preferred orientation of survivor grains in fault gouge. *Journal of Structural Geology*, 21, 419-436.
- Dowdy, S. and Wearden, S., 1991. *Statistics for Research*. John Wiley & Sons, New York, Chichester, Brisbane, Toronto, Singapore, 629 pp.
- Engelder, J.T., 1974. Cataclasis and the Generation of Fault Gouge. *GSA Bulletin*, 85, 1515-1522.
- Engelder, T., 1987. Joints and some fractures in rocks. In: Atkinson, B.K. (Ed.), *Fracture Mechanics of Rock*. Academic Press, pp. 27-69.
- Field, A., 2005. *Discovering Statistics Using SPSS*. SAGE Publications, London Thousand Oaks New Delhi, 779 pp.
- Grady, D.E. and Kipp, M.E., 1987. Dynamic rock fragmentation. *Academic Press Inc.*, London, 1987, 420-475.
- Grasemann, B., Schneider, D.A., Stöckli, D.F. and Iglseeder, C., 2011. Miocene bivergent crustal extension in the Aegean: Evidence from the western Cyclades (Greece). *Lithosphere*, 4, doi:10.1130/L164.1.
- Guo, Y., and J. K. Morgan, 2004. Influence of normal stress and grain shape on granular friction: Results of discrete element simulations. *Journal of Geophysical Research*, 109, doi: 10.1029/2004JB003044.
- Hartman, W. K., 1969. Terrestrial, lunar and interplanetary rock fragmentation. *Icarus*, 10, 201-213.
- Hausegger, S., Kurz, W., Rabitsch, R., Kiechel E. and Brosch F.-J., 2010. Analysis of the internal structure of a carbonate damage zone: Implications for the mechanisms of fault breccia formation and fluid flow. *Journal of Structural Geology*, 32, 1349-1362.
- Hattori, I. and Yamamoto, H., 1999. Rock Fragmentation and Particle Size in Crushed Zones by Faulting. *The Journal of Geology*, 107, 209-222.
- Heilbronner, R. and Keulen, N., 2006. Grain size and grain shape analysis of fault rocks. *Tectonophysics*, 427, 199-216.
- Hergarten, S., 2002. *Self-Organized Criticality in Earth Systems*. Springer-Verlag, Berlin, Heidelberg, New Yourk, 272 pp.
- Huitson, A., 1966. *The Analysis of Variance*, Number eighteen of Griffin's Statistical Monographs & Courses. Charles Griffin & Company Limited, London, 83 pp.
- Iglseeder, C., Grasemann, B., Rice, A.H.N., Petrakakis, K. and Schneider, D.A., 2011. Miocene south directed low-angle normal fault evolution on Kea Island (West Cycladic Detachment System, Greece). *Tectonics*, 30, 10.1029/2010tc002802.
- Jolivet, L. and Brun, J.-P., 2010. Cenozoic geodynamic evolution of the Aegean. *International Journal of Earth Sciences*, 99, 109-138.
- Keulen, N., Heilbronner, R., Stunitz, H., Boullier, A.-M. and Ito, H., 2007. Grain size distributions of fault rocks: A comparison between experimentally and naturally deformed granitoids. *Journal of Structural Geology*, 29, 1282-1300.
- Mair, K., Marone, C., 1999. Friction of simulated fault gouge for a wide range of velocities and normal stresses. *Journal of Geophysical Research*, 104, 28899-28914.
- Mair, K., Frye, K.M. and Marone, C., 2002. Influence of grain characteristics on the friction of granular shear zones. *Journal of Geophysical Research*, 107, 10.1029/2001jb000516.
- Marone, C. and Scholz, C.H., 1989. Particle-size distribution and microstructures within simulated fault gouge. *Journal of Structural Geology*, 11, 799-814.
- Monzawa, N. and Otsuki, K., 2003. Comminution and fluidization of granular fault materials: implications for fault slip behavior. *Tectonophysics*, 367, 127-143.
- Panazzo, R. and Hurlimann, H., 1983. A simple method for the quantitative discrimination of convex-concave lines. *Microscopica Acta* 87, 169-176.
- Passchier, C.W. and Trouw, R.A.J., 1996. *Microtectonics*. Springer-Verlag, Berlin, Heidelberg, New York, 289 pp.
- Ramsay, J.G. and Huber, I.M., 1987. *The Techniques of Modern Structural Geology*. Volume 2: Folds and Fractures. Academic Press Inc. Ltd, London, 391 pp.
- Ramsay, J.G. and Lisle, R.J., 2000. *The Techniques of Modern Structural Geology*. Volume 3: Applications of Continuum Mechanics in Structural Geology. Academic Press Inc. Ltd, London, 360 pp.
- Rawling, G.C. and Goodwin, L.B., 2003. Cataclasis and particulate flow in faulted, poorly lithified sediments. *Journal of Structural Geology*, 25, 317-331.
- Rowe, C.D., Meneghini, F. and Moore, J.C., 2011. Textural record of the seismic cycle: strain-rate variation in an ancient subduction thrust. *Geological Society, London, Special Publications*, 359, 77-95.
- Sammis, C.G., Osborne, R.H., Anderson, J.L., Badert, M. and White, P., 1986. Self-similar Cataclasis in the Formation of Fault Gouge. *Pure and Applied Geophysics*, 124, 53-78.
- Storti, F., Billi, A. and Salvini, F., 2003. Particle size distribution in natural carbonate fault rocks; insights for non-self-similar cataclasis. *Earth and Planetary Science Letters*, 206 (1-2), 173-186.

Storti, F., Balsamo, F. and Salvini, F., 2007. Particle shape evolution in natural carbonate granular wear material. *Terra Nova*, 19, 344-352.

Stünitz, H., Keulen, N., Hirose, T. and Heilbronner, R., 2010. Grain size distribution and microstructures of experimentally sheared granitoid gouge at coseismic slip rates - Criteria to distinguish seismic and aseismic faults? *Journal of Structural Geology*, 32, 59-69.

Tschegg, C. and Grasemann, B., 2009. Deformation and alteration of a granodiorite during low-angle normal faulting (Serifos, Greece). *Lithosphere*, 1, 139-154.

Wang, W. and Scholz, C.H., 1994. Wear processes during frictional sliding of a rock: A theoretical and experimental study. *Journal of Geophysical Research*, 99, 6789-6799.

Received: 17 January 2012

Accepted: 29 March 2012

Norbert KOHLMAYER¹ & Bernhard GRASEMANN

Department of Geodynamics and Sedimentology, University of Vienna,
Althanstraße 14, Vienna, Austria;

¹ Corresponding author, norbert.kohlmayer@aon.at